Eur. Phys. J. Appl. Phys. (2013) 64: 24516
DOI: 10.1051/epjap/2013120444

THE EUROPEAN PHYSICAL JOURNAL APPLIED PHYSICS

Regular Article

Subproblem approach for modeling multiply connected thin regions with an h-conformal magnetodynamic finite element formulation*

Vuong Quoc Dang[1,a], Patrick Dular[1,2], Ruth V. Sabariego[1], Laurent Krähenbühl[3], and Christophe Geuzaine[1]

[1] University of Liège, Department of Electrical Engineering and Computer Science, ACE, 4000 Liège, Belgium
[2] Fonds de la Recherche Scientifique – F.R.S.-FNRS, 1000 Brussels, Belgium
[3] University of Lyon, Ampère (CNRS UMR5005), École Centrale de Lyon, 69134 Écully Cedex, France

Received: 3 October 2012 / Received in final form: 6 May 2013 / Accepted: 9 July 2013
Published online: 8 November 2013 – © EDP Sciences 2013

Abstract. A subproblem $\boldsymbol{h}$-conformal eddy current finite element method is proposed for correcting the inaccuracies inherent to thin shell models. Such models replace volume thin regions by surfaces but neglect border effects in the vicinity of their edges and corners. The developed surface-to-volume correction problem is defined as a step of the multiple subproblems that can split a complete problem, consisting of inductors and magnetic or conducting regions, some of these being thin regions. The general case of multiply connected thin regions is considered.

1 Introduction

Thin shell (TS) finite element (FE) models [1–3], assume that the fields in the thin regions are approximated by a priori 1-D analytical distributions along the shell thickness. In a FE context, their interior is thus not meshed and is rather extracted from the studied domain, being reduced to a zero-thickness double layer with ad hoc interface conditions (ICs) linked to the inner analytical distributions. Corner and edge effects are therefore neglected.

The subproblem method (SPM) allows to correct such inaccuracies by means of surface-to-volume local corrections. Already proposed for the $\boldsymbol{h}$-conformal FE formulation and simply connected TS regions [4], the method is herein extended to multiply connected TS regions, i.e., regions with holes, for both the associated surface model (alternative to the method in [3,5]) and its volume correction. The global currents flowing around the holes and their associated voltages are naturally coupled to the local quantities, via some cuts for magnetic scalar potential discontinuities in both TS and correction SPs.

The problem at hand is split in three SPs: a reduced problem (SP u) with the inductors alone is first considered, a TS FE problem (SP p) is then added and a volume correction problem (SP k) finally replaces the TS surface FEs with volume FEs. The solution of SP u gives surface sources (SSs) for the added TS in SP p, through TS ICs [2]. Then, SSs and volume sources (VSs) in SP k allow to suppress the TS and cut discontinuities of SP p and simultaneously add the actual volume of the thin region, with its own cut discontinuity. Each SP requires a properly adapted mesh of its regions, which increases the computational efficiency.

2 Thin shell correction in the SPM

2.1 Canonical magnetodynamic problem

A canonical magnetodynamic problem i, to be solved at step i of the SPM ($i \equiv u, p$ or k), is defined in a domain Ω_i, with boundary $\partial\Omega_i = \Gamma_i = \Gamma_{h,i} \cup \Gamma_{b,i}$. The eddy current conducting part of Ω_i is denoted $\Omega_{c,i}$ and the non-conducting region is $\Omega_{c,i}^C$, with $\Omega_i = \Omega_{c,i} \cup \Omega_{c,i}^C$. Stranded (multifilamentary) inductors belong to $\Omega_{c,i}^C$, whereas massive inductors belong to $\Omega_{c,i}$. The equations, material relations and boundary conditions (BCs) of SP i are

$$\operatorname{curl} \boldsymbol{h}_i = \boldsymbol{j}_i\,,\ \operatorname{div} \boldsymbol{b}_i = 0\,,\ \operatorname{curl} \boldsymbol{e}_i = -\partial_t \boldsymbol{b}_i, \qquad \text{(1a-b-c)}$$

$$\boldsymbol{b}_i = \mu_i \boldsymbol{h}_i + \boldsymbol{b}_{s,i}\,,\ \boldsymbol{e}_i = \sigma_i^{-1} \boldsymbol{j}_i + \boldsymbol{e}_{s,i}, \qquad \text{(2a-b)}$$

$$\boldsymbol{n} \times \boldsymbol{h}_i|_{\Gamma_{h,i}} = \boldsymbol{j}_{f,i}\,,\ \boldsymbol{n} \times \boldsymbol{e}_i|_{\Gamma_{e,i} \subset \Gamma_{b,i}} = \boldsymbol{k}_{f,i}, \qquad \text{(3a-b)}$$

where $\boldsymbol{h}_i$ is the magnetic field, $\boldsymbol{b}_i$ is the magnetic flux density, $\boldsymbol{e}_i$ is the electric field, $\boldsymbol{j}_{s,i}$ is the electric current density, μ_i is the magnetic permeability, σ_i is the electric conductivity and $\boldsymbol{n}$ is the unit normal exterior to Ω_i. The fields $\boldsymbol{b}_{s,i}$ and $\boldsymbol{e}_{s,i}$ in (2a) and (2b) are VSs that can be

* Contribution to the Topical Issue "Numelec 2012", Edited by Adel Razek.

[a] e-mail: quocvuong.dang@ulg.ac.be

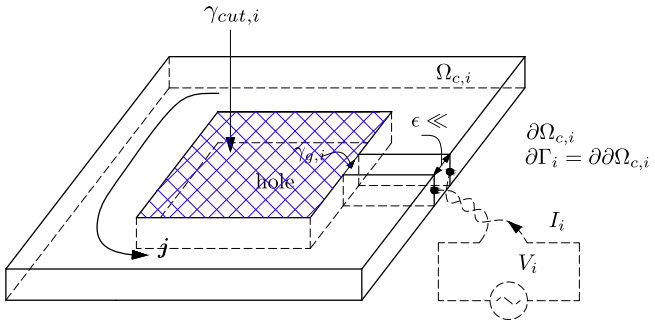

Fig. 1. 3D plate with a hole, its associated cut and source of electromotive force.

used for expressing changes of permeability or conductivity from previous SPs [6].

The surface fields $\boldsymbol{j}_{f,i}$ and $\boldsymbol{k}_{f,i}$ in (3a-b) are generally zero for classical homogeneous BCs. Some ICs can define their discontinuities through any interface γ_i (with sides γ_i^+ and γ_i^-) in Ω_i) in Ω_i, with notation $[\cdot]_{\gamma_i} = |_{\gamma_i^+} - |_{\gamma_i^-}$. If nonzero, they define possible SSs that account for particular phenomena appearing in the idealized thin region between γ_i^+ and γ_i^- [6]. A typical case appears when some field traces in a previous problem are forced to be discontinuous, whereas their continuity must be recovered via a correction problem: the SSs in SP i are then fixed as the opposite of the trace discontinuities accumulated from the previous problems.

For the magnetic field formulation, the magnetic field $\boldsymbol{h}_i$ is split into two parts, i.e., $\boldsymbol{h}_i = \boldsymbol{h}_{s,i} + \boldsymbol{h}_{r,i}$, where $\boldsymbol{h}_{s,i}$ is a source magnetic field due to the fixed current density $\boldsymbol{j}_{s,i}$ such that $\mathrm{curl}\,\boldsymbol{h}_{s,i} = \boldsymbol{j}_{s,i}$, and $\boldsymbol{h}_{r,i}$ is the reaction magnetic field. In non-conducting regions $\Omega_{c,i}^C$, field $\boldsymbol{h}_{r,i}$ is defined via a scalar potential ϕ_i, i.e., $\boldsymbol{h}_{r,i} = -\mathrm{grad}\,\phi_i$. Potential ϕ_i in a multiply connected region $\Omega_{c,i}^C$ is multivalued and is made single-valued via the definition of cuts through each hole of $\Omega_{c,i}$ [7,8] (see [9] for information on an automatic generation of cuts) (Fig. 1).

2.2 From SP u to SP p-inductor alone to TS model

The solution of an SP u is first known for an inductor alone (Fig. 2a). The next SP p consists in adding a TS to SP u (Fig. 2b). SP p is constrained via a SS, that is related to the BCs and ICs given by the TS model [2], to be combined with contributions from SP u.

With the TS model, a volume shell initially in $\Omega_{c,i}$ is extracted from Ω_i and then replaced by the double layer TS surface γ_p [2]. The TS model for the magnetic field formulation [2] involves the unknown discontinuity of $\boldsymbol{h}_{d,p}$ of the tangential component $\boldsymbol{h}_{t,p} = (\boldsymbol{n} \times \boldsymbol{h}_p) \times \boldsymbol{n}$ of $\boldsymbol{h}_p$ on the TS γ_p, i.e.,

$$[\boldsymbol{h}_p]_{\gamma_p} = \boldsymbol{h}_{d,p} \;\text{ or }\; [\boldsymbol{n} \times \boldsymbol{h}_p]_{\gamma_p} = \boldsymbol{n} \times \boldsymbol{h}_{d,p}, \tag{4}$$

fixed to zero along the TS border to prevent any current flow through it. In order to explicitly express this discontinuity, the field $\boldsymbol{h}_p$ is written on both sides of γ_p as

$$\boldsymbol{h}_p|_{\gamma_p^+} = \boldsymbol{h}_{c,p} + \boldsymbol{h}_{d,p}\,,\;\; \boldsymbol{h}_p|_{\gamma_p^-} = \boldsymbol{h}_{c,p}, \tag{5 a-b}$$

where $\boldsymbol{h}_{c,p}$ is the continuous component of $\boldsymbol{h}_p$. Definitions (5a-b) also apply on γ_p for the tangential components $\boldsymbol{h}_{t,p}$, $\boldsymbol{h}_{c,t,p}$ and $\boldsymbol{h}_{d,t,p}$.

TS discontinuities also exist for the scalar potential ϕ_p, i.e., $[\phi_p]_{\gamma_p} = \Delta\phi_p|_{\gamma_p} = \phi_{d,p}|_{\gamma_p}$ (Fig. 3), also writing $\phi_p|_{\gamma_p^+} = \phi_{c,p}|_{\gamma_p} + \phi_{d,p}|_{\gamma_p}$ and $\phi_p|_{\gamma_p^-} = \phi_{c,p}|_{\gamma_p}$ with continuous and discontinuous components of ϕ_p.

Scalar potential discontinuities $\phi_{d,p}$ of ϕ_p appear as well through the cuts making $\Omega_{c,p}^C$ single-valued, being cut-wise constant, i.e.,

$$\begin{aligned}[\phi_p]_{\gamma_{\mathrm{cut},p}} = \Delta\phi_p|_{\gamma_{\mathrm{cut},p}} &= \phi_p|_{\gamma_{\mathrm{cut},p}^+} - \phi_p|_{\gamma_{\mathrm{cut},p}^-} \\ &= \phi_{d,p}|_{\gamma_{\mathrm{cut},p}} = I_{\mathrm{cut},p},\end{aligned} \tag{6}$$

where $I_{\mathrm{cut},p}$ is the global current flowing around each cut [10].

Discontinuities $\phi_{d,p}|_{\gamma_p}$ and $\phi_{d,p}|_{\gamma_{\mathrm{cut},p}}$ have to be matched at the TS-cuts intersections.

With the TS model, the continuous and discontinuous components of the current total primal unknown $\boldsymbol{h} = \boldsymbol{h}_u + \boldsymbol{h}_p$ [2], i.e.,

$$\boldsymbol{h}_c = \boldsymbol{h}_u + \boldsymbol{h}_{c,p}, \quad \boldsymbol{h}_d = \boldsymbol{h}_{d,p}, \tag{7}$$

are involved in the expression of the trace discontinuity IC $[\boldsymbol{n} \times \boldsymbol{e}_p]_{\gamma_p}$ via

$$[\boldsymbol{n} \times \boldsymbol{e}]_{\gamma_p} = [\boldsymbol{n} \times \boldsymbol{e}_u]_{\gamma_p} + [\boldsymbol{n} \times \boldsymbol{e}_p]_{\gamma_p} = \mu_p \beta_p\, \partial_t (2\boldsymbol{h}_c + \boldsymbol{h}_d), \tag{8}$$

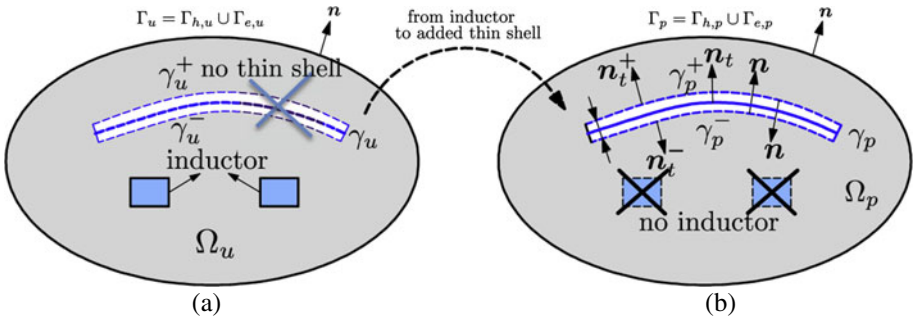

Fig. 2. Regions defining SP u and SP p.

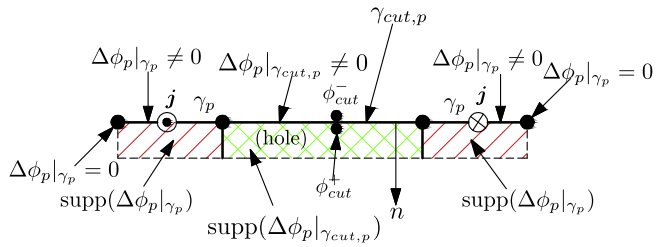

Fig. 3. Section of a 3D plate with a hole, with the associated cut and transition layer (supp) for $\Delta\phi_p$.

$$\beta_p = \theta_p^{-1}\tanh(d_p\theta_p/2), \theta_p = (1+\jmath)/\delta_p, \tag{9}$$

where d_p is the local TS thickness, $\delta_p = \sqrt{2/\omega\sigma_p\mu_p}$ is the skin depth in the TS, $\omega = 2\pi f$, f is the frequency and $\jmath$ is the imaginary unit. The term $[\boldsymbol{n}\times\boldsymbol{e}_u]_{\gamma_p}$ in (8) is zero because there are no discontinuity in SP u (before adding γ_p). Also, the trace of $\boldsymbol{e}_p$ on the positive side γ_p^+ is expressed as [2]:

$$\begin{aligned}\boldsymbol{n}\times\boldsymbol{e}_p|_{\gamma_p^+} &= \boldsymbol{n}\times\boldsymbol{e}|_{\gamma_p^+} - \boldsymbol{n}\times\boldsymbol{e}_u|_{\gamma_p^+}\\ &= \frac{1}{2}\big[\mu_p\beta_p\,\partial_t(2\boldsymbol{h}_c+\boldsymbol{h}_d) + \frac{1}{\sigma_p\beta_p}\,\boldsymbol{h}_d\big]\\ &\quad -\boldsymbol{n}\times\boldsymbol{e}_u|_{\gamma_p^+}.\end{aligned} \tag{10}$$

2.3 From SP p to SP k-TS model to volume model

The TS solution obtained in SP p is then corrected by means of SP k that overcomes the TS assumptions. The SPM offers the tools to perform such a model refinement, thanks to simultaneous SSs and VSs. A volume mesh of the shell is now required and extended to its neighborhood without including the other regions of previous SPs. This allows to focus on the fineness of the mesh only in the shell and its neighborhood. SP k has to suppress the TS representation via SSs opposed to TS discontinuities, in parallel to VSs in the added volume shell [4] that accounts for volume changes of μ_p and σ_p in SP p to μ_k and σ_k in SP k (with $\mu_p = \mu_0$, $\mu_k = \mu_{\text{volume}}$, $\sigma_p = 0$ and $\sigma_k = \sigma_{\text{volume}}$). This correction can be limited to the neighborhood of the shell, which permits to benefit from a reduction of the extension of the associated mesh [4]. The VSs for SP k are [4,6]:

$$\boldsymbol{b}_{s,k} = (\mu_k-\mu_p)(\boldsymbol{h}_u+\boldsymbol{h}_p), \quad \boldsymbol{e}_{s,k} = -(\boldsymbol{e}_u+\boldsymbol{e}_p). \tag{11a-b}$$

3 Finite element weak formulations

3.1 h − Formulation with source and reaction magnetic fields

The $\boldsymbol{h}_i$-ϕ_i formulation of SP i ($i \equiv u$, p or k) is obtained from the weak form of Faraday's law (1 c) [6], i.e.,

$$\begin{aligned}&\partial_t(\mu_i(\boldsymbol{h}_{r,i}+\boldsymbol{h}_{s,i}),\boldsymbol{h}'_i)_{\Omega_i} + (\sigma_i^{-1}\operatorname{curl}\boldsymbol{h}_i,\operatorname{curl}\boldsymbol{h}'_i)_{\Omega_{c,i}}\\ &+\partial_t(\boldsymbol{b}_{s,i},\boldsymbol{h}'_i)_{\Omega_i} + (\boldsymbol{e}_{s,i},\operatorname{curl}\boldsymbol{h}'_i)_{\Omega_i} + \langle[\boldsymbol{n}\times\boldsymbol{e}_i]_{\gamma_i},\boldsymbol{h}'_i\rangle_{\gamma_i}\\ &+\langle\boldsymbol{n}\times\boldsymbol{e}_i,\boldsymbol{h}'_i\rangle_{\Gamma_{e,i}} = 0, \forall\boldsymbol{h}'_i\in F_i^1(\Omega_i),\end{aligned} \tag{12}$$

where $F_i^1(\Omega_i)$ is a curl-conform function space defined in Ω_i and contains the basis functions for $\boldsymbol{h}_i$ (coupled to ϕ_i) as well as for the test function $\boldsymbol{h}'_i$; $(\cdot,\cdot)_{\Omega_i}$ and $<\cdot,\cdot>_{\Gamma_i}$ respectively, denote a volume integral in Ω_i and a surface integral on Γ_i of the product of their vector field arguments. The surface integral term on $\Gamma_{e,i}$ accounts for natural BCs of type (3b), usually zero. At the discrete level, the required meshes for each SP i differ.

3.2 Inductor model−SP u

The model SP u with only the inductor is first solved with (12) ($i \equiv u$). The source field $\boldsymbol{h}_{s,u}$ is defined via a projection method of a known distribution $\boldsymbol{j}_{s,u}$ [11], i.e.,

$$\begin{aligned}(\operatorname{curl}\boldsymbol{h}_{s,u},\operatorname{curl}\boldsymbol{h}'_{s,u})_{\Omega_u} &= (\boldsymbol{j}_{s,u},\operatorname{curl}\boldsymbol{h}'_{s,u})_{\Omega_{s,u}},\\ \forall\boldsymbol{h}'_{s,u}&\in F_u^1(\Omega_u).\end{aligned} \tag{13}$$

3.3 Thin shell FE model−SP p

The TS model is defined via the term $\langle[\boldsymbol{n}\times\boldsymbol{e}_p]_{\gamma_p},\boldsymbol{h}'_p\rangle_{\gamma_p}$ in (12) ($i \equiv p$). The test function $\boldsymbol{h}'_p$ is split into continuous and discontinuous parts $\boldsymbol{h}'_c$ and $\boldsymbol{h}'_d$ [2]. One thus has

$$\begin{aligned}\langle[\boldsymbol{n}\times\boldsymbol{e}_p]_{\gamma_p},\boldsymbol{h}'_p\rangle_{\gamma_p} &= \langle[\boldsymbol{n}\times\boldsymbol{e}_p]_{\gamma_p},\boldsymbol{h}'_c+\boldsymbol{h}'_d\rangle_{\gamma_p}\\ &= \langle[\boldsymbol{n}\times\boldsymbol{e}_p]_{\gamma_p},\boldsymbol{h}'_c\rangle_{\gamma_p} + \langle[\boldsymbol{n}\times\boldsymbol{e}_p]_{\gamma_p},\boldsymbol{h}'_d\rangle_{\gamma_p},\end{aligned} \tag{14}$$

with $\boldsymbol{h}'_d$ zero on γ_p^-. Thus (14) becomes

$$\begin{aligned}\langle[\boldsymbol{n}\times\boldsymbol{e}_p]_{\gamma_p},\boldsymbol{h}'_p\rangle_{\gamma_p} &= \langle[\boldsymbol{n}\times\boldsymbol{e}_p]_{\gamma_p},\boldsymbol{h}'_c\rangle_{\gamma_p}\\ &\quad + \left\langle\boldsymbol{n}\times\boldsymbol{e}_p|_{\gamma_p^+},\boldsymbol{h}'_d\right\rangle_{\gamma_p^+}.\end{aligned} \tag{15}$$

The terms of the RHS of (15) are developed using (8) and (10) respectively, i.e.,

$$\begin{aligned}\langle[\boldsymbol{n}\times\boldsymbol{e}_p]_{\gamma_p},\boldsymbol{h}'_c\rangle_{\gamma_p} &= \langle[\boldsymbol{n}\times\boldsymbol{e}]_{\gamma_p},\boldsymbol{h}'_c\rangle_{\gamma_p}\\ &= \langle\mu_p\beta_p\,\partial_t(2\boldsymbol{h}_c+\boldsymbol{h}_d),\boldsymbol{h}'_c\rangle_{\gamma_p},\end{aligned} \tag{16}$$

$$\begin{aligned}&\left\langle\boldsymbol{n}\times\boldsymbol{e}_p|_{\gamma_p^+},\boldsymbol{h}'_d\right\rangle_{\gamma_p}\\ &= \left\langle\frac{1}{2}\big[\mu_p\beta_p\,\partial_t(2\boldsymbol{h}_c+\boldsymbol{h}_d)+\frac{1}{\sigma_p\beta_p}\,\boldsymbol{h}_d\big],\boldsymbol{h}'_d\right\rangle_{\gamma_p}\\ &\quad -\left\langle\boldsymbol{n}\times\boldsymbol{e}_u|_{\gamma_p^+},\boldsymbol{h}'_d\right\rangle_{\gamma_p}.\end{aligned} \tag{17}$$

The last surface integral term in (17) is related to a SS that can be naturally expressed via the weak formulation of SP u (12), i.e.,

$$-\left\langle\boldsymbol{n}\times\boldsymbol{e}_u|_{\gamma_p^+},\boldsymbol{h}'_d\right\rangle_{\gamma_p^+} = (\mu_u\partial_t(\boldsymbol{h}_{s,u}+\boldsymbol{h}_{r,u}),\boldsymbol{h}'_d)_{\Omega_p^+}. \tag{18}$$

At the discrete level, the volume integral in (18) is thus limited to a single layer of FEs on the side Ω_p^+ touching γ_p+, because it involves only the associated trace $\boldsymbol{n}\times\boldsymbol{h}'_d|_{\gamma_p^+}$. Also, the source $\boldsymbol{h}_u$, initially in the mesh of SP u, has to be projected on the mesh of SP p [4,6], using a projection method [11]. The projection can be limited to the particular region $\Omega_{s,p}$ where the field is used as a source, in this case in the single layer Ω_p^+. One has

$$(\boldsymbol{h}_{u,p\text{-proj}},\boldsymbol{h}')_{\Omega_{s,p}}=(\boldsymbol{h}_u,\boldsymbol{h}')_{\Omega_{s,p}},\forall\boldsymbol{h}'\in F_p^1(\Omega_{s,p}),\quad(19)$$

where $F_p^1(\Omega_{s,p})$ is a gauged curl-conform function space for the p-projected source $\boldsymbol{h}_{u,p\text{-proj}}$ (the projection of $\boldsymbol{h}_u$ on mesh p) and the test function $\boldsymbol{h}'$.

3.4 Volume correction replacing the thin shell representation−SP k

Once obtained, the TS solution in SP p is corrected by SP k via VSs given in (11a-b). These VSs are taken into account in (12) ($i\equiv k$) via the volume integrals $(\boldsymbol{e}_{s,k},\operatorname{curl}\boldsymbol{h}'_k)_{\Omega_k}$ and $\partial_t(\boldsymbol{b}_{s,k},\boldsymbol{h}'_k)_{\Omega_k}$. The VS $\boldsymbol{e}_{s,k}$ in (11b) is to be obtained from the still unknown electric fields $\boldsymbol{e}_u$ and $\boldsymbol{e}_p$. They are unknown in $\Omega_{c,p}^C$ and their determination requires to solve an electric problem [6].

Simultaneously to the VSs in (12), ICs compensate the TS and cut discontinuities, i.e., $\phi_{d,p}|_{\gamma_p}$ and $\phi_{d,p}|_{\gamma_{\text{cut},p}}$, and $[\boldsymbol{n}\times\boldsymbol{e}_p]_{\gamma_p}$, to suppress the TS representation via SSs opposed to previous TS ICs, i.e., $\boldsymbol{h}_{d,k}=-\boldsymbol{h}_{d,p}$ and $\phi_{d,k}=-\phi_{d,p}$ to be strongly defined, and $[\boldsymbol{n}\times\boldsymbol{e}_k]_{\gamma_k}=-[\boldsymbol{n}\times\boldsymbol{e}_p]_{\gamma_k}$. The trace discontinuity $[\boldsymbol{n}\times\boldsymbol{e}_k]_{\gamma_k}$ occurs in (12) via

$$\left\langle[\boldsymbol{n}\times\boldsymbol{e}_k]_{\gamma_k},\boldsymbol{h}'_k\right\rangle_{\gamma_k}=-\left\langle[\boldsymbol{n}\times\boldsymbol{e}_p]_{\gamma_k},\boldsymbol{h}'_k\right\rangle_{\gamma_k},\quad(20)$$

and can be weakly evaluated from a volume integral from SP p similarly to (18). However, directly using the explicit form (8) for $[\boldsymbol{n}\times\boldsymbol{e}_p]_{\gamma_k}$ gives the same contribution, which is thus preferred. For that, it is enough to project fields $\boldsymbol{h}_u$, $\boldsymbol{h}_{c,p}$ and $\boldsymbol{h}_{d,p}$ on γ_k, on which (7) is then evaluated.

3.5 Global quantities in TS and volume models

The surface integral $\left\langle\boldsymbol{n}\times\boldsymbol{e}_i,\boldsymbol{h}'_i\right\rangle_{\Gamma_{e,i}}$ in (12) can be extended to a global condition weakly defining a voltage V_i [10], with $\boldsymbol{h}'_i=\boldsymbol{c}_i=-\operatorname{grad}q_i$ in $\Omega_{c,i}^C$ with $\boldsymbol{n}\times\boldsymbol{c}_i=-\boldsymbol{n}\times\operatorname{grad}q_i$ on $\partial\Omega_{c,i}$ ($\boldsymbol{c}_i$ is the current basis function) made simply connected by the cut γ_i (Figs. 1 and 3). Potential q_i is fixed to 1 on one side of the cut and to 0 on the other side. The continuous transition of q_i between these values can be performed in a transition layer in $\Omega_{c,i}^C$ adjacent to side "+" (Figs. 1 and 3), which reduces the support of q_i and $\boldsymbol{c}_i$. One gets [10]

$$\langle\boldsymbol{n}\times\boldsymbol{e}_i,\boldsymbol{c}_i\rangle_{\partial\Omega_{c,i}}=\oint_{\partial\Gamma_i}q_i\boldsymbol{e}_i\,\mathrm{d}l=\int_{\gamma_{g,i}}\boldsymbol{e}_i\,\mathrm{d}l=V_i,\quad(21)$$

where $\gamma_{g,i}$ is a path connecting two real or imaginary electrodes of the thin region. The global current I_i is strongly defined by (6).

3.6 Discretization of the reaction magnetic field

At the discrete level, the use of edge FEs [2] to interpolate curl-conform fields, such as the magnetic field $\boldsymbol{h}_i$, first gives facilities in defining currents. Indeed, the circulation of such fields along a closed path, also being the flux of its curl and consequently the current, is directly obtained from coefficients of the interpolation, in this case those associated with the edges of the path [12].

The magnetic field $\boldsymbol{h}_i$ in (12) is thus discretized by edge FEs, generating the function space $\in S_i^1(\Omega_i)$ defined on a mesh of Ω_i [2,10,12], i.e.,

$$\boldsymbol{h}_i=\sum_{e\in E(\Omega_i)}h_{e,i}s_{e,i},\quad\forall\boldsymbol{h}_i\in S_i^1(\Omega_i),\quad(22)$$

where $E(\Omega_i)$ is the set of edges of Ω_i, $s_{e,i}$ is the edge basis function associated with edge e and $h_{e,i}$ is the circulation of $\boldsymbol{h}_i$ along the edge e. Now, characterization (22) can be transformed in order to give explicitly the basis functions of the considered discrete space for $F_i^1(\Omega_i)$ with the essential constraint, i.e., $\boldsymbol{h}_{r,i}=-\operatorname{grad}\phi_i$, using the results of [10,12]. One has

$$\begin{aligned}\boldsymbol{h}_i=&\sum_{e\in E(\Omega_{c,i}\setminus\partial\Omega_{c,i})}h_{e,i}s_{e,i}+\sum_{n\in N(\Omega_{c,i}^C)}\phi_{c,n,i}\,v_{c,n,i}\\&+\sum_{n\in N(\gamma_i)}\phi_{d,i}\,t_{d,n,i}+I_{\text{cut},i}\sum_{n\in N(\gamma_{\text{cut},i})}c_{d,n,i},\end{aligned}\quad(23)$$

where $N(\cdot)$ is the sets of nodes of the mesh of a given region. Coefficients I_{c_i} represent circulations of $\boldsymbol{h}_i$ along well-defined paths given by (6). The functions $t_{d,n,i}$ and $c_{d,n,i}$ can be respectively expressed in the thin regions and the cuts as [2]

$$t_{d,n,i}=\begin{cases}\displaystyle\sum_{\substack{\{n,m\}\in E(\Omega_{c,i}^C)\\ n\in N(\Gamma_{ts,i})\\ m\notin N(\Gamma_{ts,i})\\ m\in N_{ts,i}^+}}s_{e,\{n,m\}}&\text{in supp}\,(\Delta\phi_i|_{\Gamma_{ts,i}})\\ 0&\text{otherwise,}\end{cases},$$

$$c_{d,n,i}=\begin{cases}\displaystyle\sum_{\substack{\{n,m\}\in E(\Omega_{c,i}^C)\\ n\in N(\Gamma_{\text{cut},i})\\ m\notin N(\Gamma_{\text{cut},i})\\ m\in N_{\text{cut},i}^+}}s_{e,\{n,m\}}&\text{in supp}\,(\Delta\phi_i|_{\Gamma_{\text{cut},i}})\\ 0&\text{otherwise,}\end{cases},$$

where $m\in N_{ts,i}^+$ and $m\in N_{\text{cut},i}^+$ are the sets of nodes of the transition layers supp $(\Delta\phi_i|_{\Gamma_{ts,i}})$ and supp $(\Delta\phi_i|_{\Gamma_{\text{cut},i}})$, respectively (Fig. 3).

4 Application

The 3D test problem is based on TEAM problem 7: an inductor placed above a thin plate with a hole (Fig. 4)

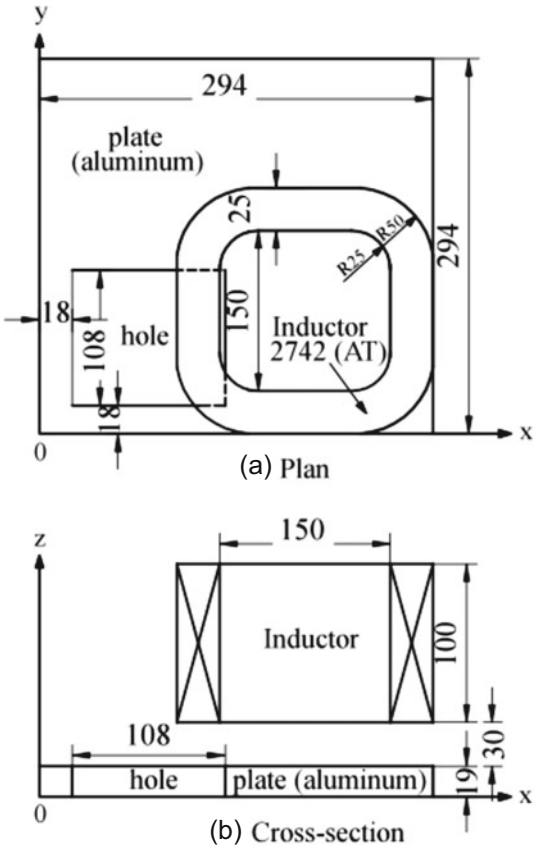

Fig. 4. Geometry of TEAM problem 7: inductor and conducting plate with a hole (all dimensions are in mm).

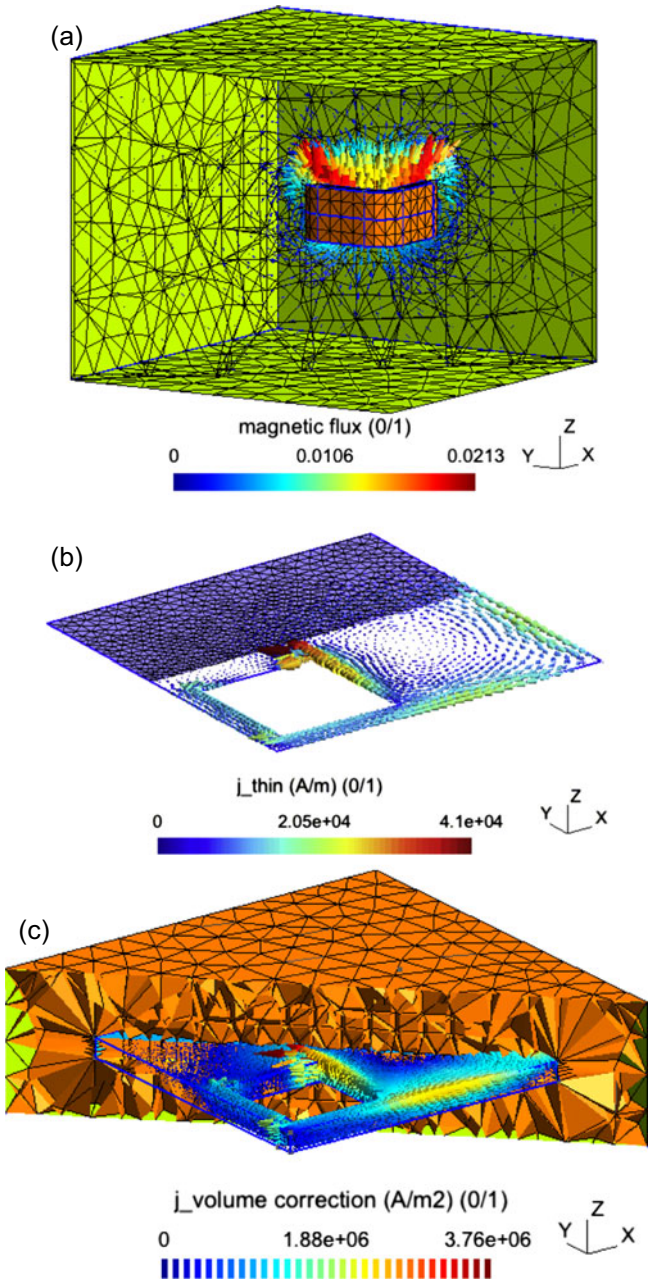

Fig. 5. TEAM problem 7: magnetic flux density $\boldsymbol{b}_u$ (in a cut plane) generated by a stranded inductor (a), TS eddy current density $\boldsymbol{j}_p$ (b) and its volume correction (locally focussing on the mesh of plate and its neighborhood) $\boldsymbol{j}_k$ (c) ($d = 19$ mm, $f = 200$ Hz).

($\mu_r = 1$, $\sigma_{\text{plate}} = 35.26$ MS/m). A magnetodynamic SP scheme considering three SPs is proposed. A first FE SP u with the stranded inductor alone is solved on a simplified mesh without any thin regions (Fig. 5a). Then, an SP p is solved with the added thin region via a TS FE model (Fig. 5b); the surface TS is located on the inductor side of the actual volume shell, which makes the TS error smaller in this case. An SP k eventually replaces the TS FEs with the volume FEs covering the actual plate and its neighborhood with an adequate refined mesh (Fig. 5c). The TS error on $\boldsymbol{j}_p$ locally reaches 50% (Fig. 5b), with plate thickness $d = 19$ mm and frequency $f = 200$ Hz (skin depth $\delta = 6$ mm). The inaccuracy on the Joule power loss densities of TS SP p is pointed out by the importance of the correction SP k (Figs. 6 and 7). It reaches several tens of percents along the plate borders and near the plate ends for some critical parameters: e.g., 28% (Fig. 6a) and 32% (Fig. 7a), with $f = 50$ Hz and $\delta = 11.98$ mm in both case, or 53% (Fig. 6b) and 61% (Fig. 7b), with $f = 200$ Hz and $\delta = 6$ mm in both cases. Accurate local corrections with SP k are checked to be close to the reference or complete FE solution (Fig. 8), with errors being lower than 0.01%. The errors particularly decrease with a smaller thickness ($d = 2$ mm), being lower than 15% (Fig. 9), with $f = 200$ Hz and $\delta = 6$ mm.

Significant errors on the Joule losses and the global currents flowing around the hole between TS SP p and volume correction SP k are shown in Table 1. For $d = 19$ mm and $f = 200$ Hz, the TS error is 14% for the global

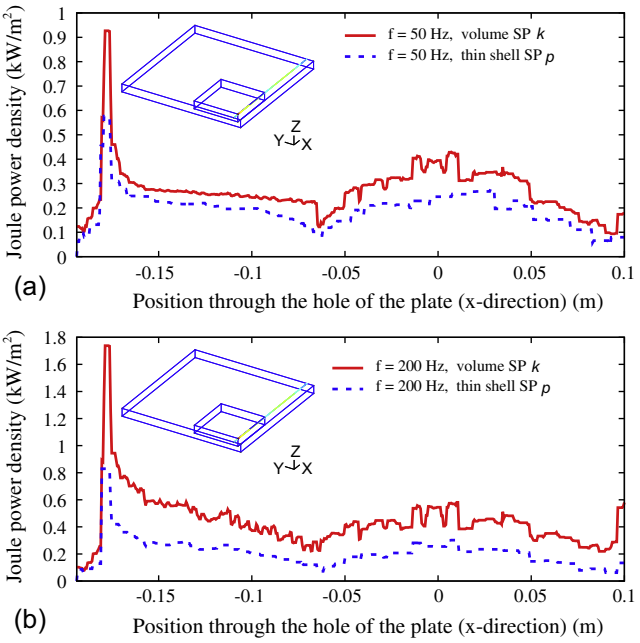

Fig. 6. Joule power loss density with TS model and volume correction along hole and plate borders (along the line drawn in the plate geometry) ($d = 19$ mm).

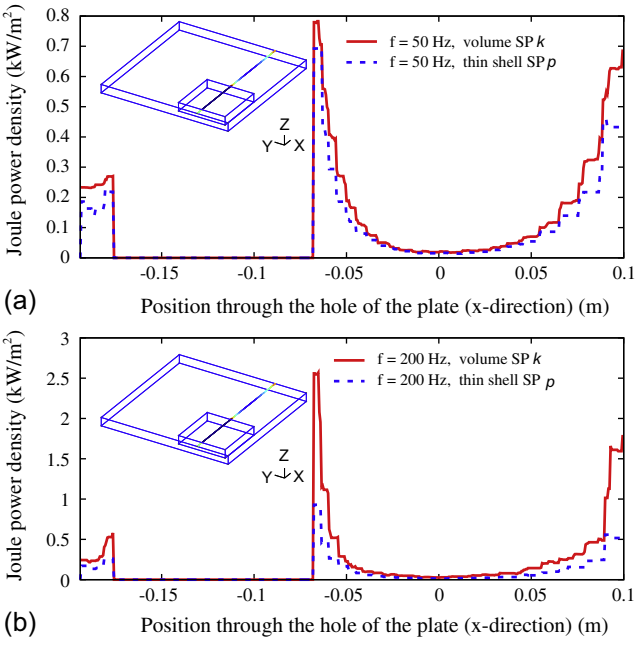

Fig. 7. Joule power loss density with TS model and volume correction through the hole ($d = 19$ mm).

current and 41.51% for the Joule losses (reduced to 26.18% for $f = 50$ Hz). For $d = 2$ mm and $f = 200$ Hz, it is respectively reduced to 1.1% and 6.44% (4.36% for $f = 50$ Hz).

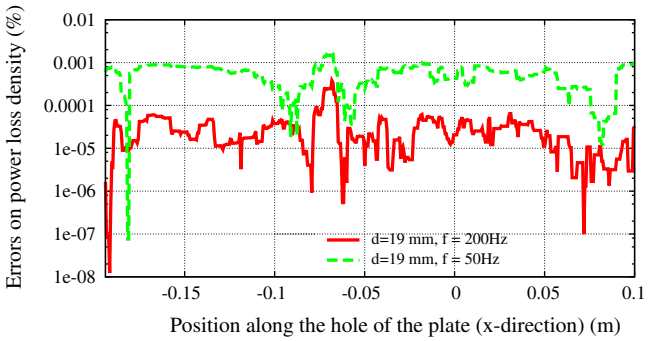

Fig. 8. Error on the power loss density between volume correction and reference problem along hole and plate borders.

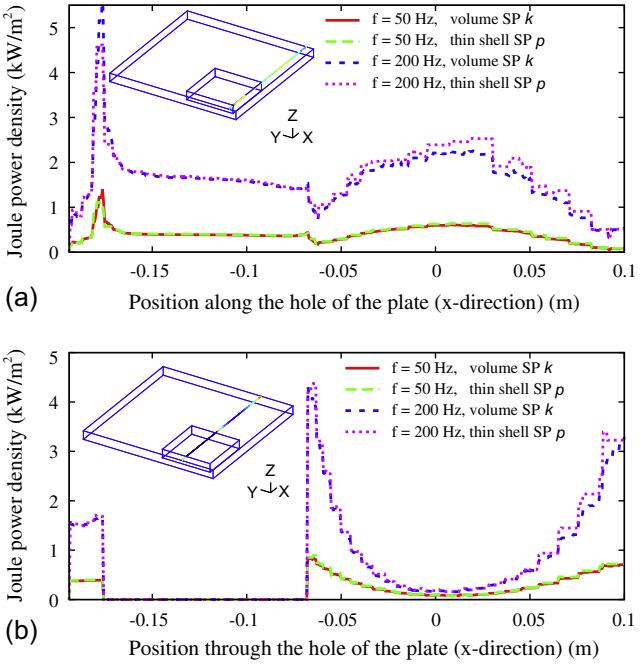

Fig. 9. Joule power loss density with TS model and volume correction along hole and plate borders (a), and through the hole (b) ($d = 2$ mm).

Table 1. Joule losses and global currents (with errors between TS SP p and volume correction SP k).

Joule losses in the plate				
Thickness	Frequency	Thin shell	Volume	Errors
d (mm)	f (Hz)	P_{thin} (W)	P_{vol} (W)	(%)
2	50	14.45	13.82	4.36
19	50	5.86	7.95	26.18
2	200	50.44	47.33	6.44
19	200	8.88	15.19	41.51
Global currents flowing around the hole				Errors
d (mm)	f (Hz)	I_{thin} (A)	I_{vol} (A)	(%)
2	50	94,5	93.5	1.1
19	50	173.3	199.8	13.2
2	200	190.4	186.5	1.8
19	200	179.3	206.3	14

5 Conclusions

The SPM allows to accurately correct any TS solution. In particular, accurate corrections of eddy current and power loss densities are obtained at the edges and corners of multiply connected thin regions. All the steps of the method for TS models and their corrections have been presented and validated by coupling SPs via the SPM with the $\boldsymbol{h}$-formulation. The method has been successfully applied to the TEAM problem 7.

This work was supported by the Belgium Sciency Policy (IAP 7/02 "Multiscale modelling of Electrical Energy Systems").

References

1. L. Krähenbühl, D. Muller, IEEE Trans. Magn. **29**, 1450 (1993)
2. C. Geuzaine, P. Dular, W. Legros, IEEE Trans. Magn. **36**, 799 (2000)
3. C. Guérin, G. Meunier, IEEE Trans. Magn. **48**, 323 (2012)
4. V.Q. Dang, P. Dular, R.V. Sabariego, L. Krähenbühl, C. Geuzaine, IEEE Trans. Magn. **48**, 407 (2012)
5. T. Le-Duc, G. Meunier, O. Chadebec, J.-M. Guichon, IEEE Trans. Magn. **48**, 427 (2012)
6. P. Dular, R.V. Sabariego, IEEE Trans. Magn. **43**, 1293 (2007)
7. A. Bossavit, IEE Proc. A Sci. Meas. Technol. UK **135**, 179 (1988)
8. D. Rodger, N. Atkinson, IEEE Trans. Magn. **23**, 3047 (1987)
9. P.A. Tuan, O. Chadebec, P. Labie, Y.L. Floch, G. Meunier, IEEE Trans. Magn. **41**, 1668 (2005)
10. P. Dular, W. Legros, IEEE Trans. Magn. **34**, 3078 (1998)
11. C. Geuzaine, B. Meys, F. Henrotte, P. Dular, W. Legros, IEEE Trans. Magn. **35**, 1438 (1999)
12. P. Dular, J.Y. Hody, A. Nicolet, A. Gennon, W. Legros, IEEE Trans. Magn. **30**, 2980 (1994)